主論文の要旨

Rho-Kinase/ROCK Phosphorylates PSD-93 Downstream of NMDARs to Orchestrate Synaptic Plasticity

（Rho-Kinase/ROCKはNMDA受容体の下流でPSD-93をリン酸化し、シナプス可塑性を制御する）

名古屋大学大学院医学系研究科　総合医学専攻
神経科学講座　神経情報薬理学分野
（指導：山田 清文　教授）
Emran Hossen

【Introduction】

Synaptic plasticity is a key mechanism of learning and memory. During synaptic plasticity, there is an important event occurred named long-term potentiation (LTP). LTP is crucial for strengthening connections between neurons by enlarging the dendritic spine volume. Glutamate-containing presynaptic vesicles release glutamate into the synaptic cleft upon LTP formation, which subsequently binds to postsynaptic glutamate receptors, such as α-amino-3-hydroxy-5-methyl-4-isoxazolepropionic acid receptors (AMPARs), N-methyl-D-aspartate receptors (NMDARs), and kainate receptors. Among these glutamate receptors, glutamate binds to AMPARs and increases Na^+ influx via their pores and subsequently removes Mg^{2+} from NMDARs that blocks Ca^{2+} influx upon glutamate stimulation. By removing Mg^{2+}, glutamate neurotransmitters initiate Ca^{2+} influx through the NMDARs, thereby activating CaMKII via autophosphorylation. Active CaMKII activates the RhoA–Rho-kinase cascade, which induces dendritic spine enlargement. However, the mechanism by which Rho-kinase regulates dendritic spine formation during LTP is not yet fully understood.

To identify *in vivo* Rho-kinase candidate substrates, we previously reported a novel phosphoproteomic method that uses affinity beads coated with 14-3-3 bait proteins to capture phospho-Ser/Thr containing peptides. The data obtained from phosphoproteomics were deposited in our online database, the Kinase-Associated Neural Phospho-Signaling database (KANPHOS; https://kanphos.neuroinf.jp). We hypothesized that the KANPHOS data included Rho-kinase candidate substrates that were involved in synaptic plasticity. We identified discs large MAGUK scaffold protein 2 (DLG2/PSD-93) as a Rho-kinase candidate substrate in the striatum. We found that Rho-kinase phosphorylates PSD-93 downstream of NMDARs and that Rho-kinase increases the interactions of PSD-93 with PSD-95 but decreases the interaction of PSD-93 with synaptic Ras GTPase-activating protein 1 (SynGAP1), ADAM metallopeptidase domain 22 (ADAM22), and leucine rich glioma inactivated 1 (LGI1). In conclusion, our observations improve the current understanding of how Rho-kinase regulates the interaction of synaptic proteins with NMDARs and AMPARs to orchestrate synaptic plasticity.

【Materials and Methods】

Striatal slice culture

In this method, the mice were sacrificed humanly by beheading and the brain was immediately collected in Krebs-HCO_3^- buffer. The mouse brain was coronally sliced (350 μM) using a VT1200S vibratome. Then, the striatal slices were incubated in the Krebs-HCO_3^- buffer containing 10 μg/mL adenosine deaminase (Roche) at 30°C with oxygenation (95% O_2/5% CO_2). After 30 min of incubation buffer was changed to fresh Krebs-HCO_3^- buffer, and the slices were incubated another 30 min. The striatal slices were treated with calyculin A (250 nM) for 60 min with or without Y-27632 (20 μM). After drug treatment, the striatal slices were frozen in liquid nitrogen and stored at −80°C until assayed.

Immunoprecipitation assay

The calyculin A (250 nM for 60 min) and Y-27632 (20 μM for 60 min) treated striatal slices were sonicated immediately with 320 μL of RIPA buffer. The solution was centrifuged at 16,000×g at 4°C for 10 min. The soluble supernatant was transferred to a new tube and incubated with an anti-PSD-93 antibody (1–2 μg) along with a control rabbit anti-IgG antibody (1–2 μg). The samples were gently rotated on a rotator at 4°C for 1 h. Next, 25 μL of Protein A Sepharose beads (20% ethanol) were added to each tube, and the tubes were rotated for 1 h. The proteins unbound to beads were washed out with a wash buffer and stored at -30°C until assayed.

Chemical LTP assay

In this chemical LTP assay, primary striatal neurons were dissected from E16 embryonic mice and cultured in B-27 supplemented Neurobasal medium™. After DIV21, the neurons were treated with Y-27632, then incubated with nACSF solution for 10 min. Next, the medium was changed to 200 μM glycine containing nACSF and incubated for 5 min. Finally, the neurons were incubated with the original Neurobasal Medium™ for 10 min and 60 min. The neurons were collected with 1xSDS and boiled for Immunoblot assay or fixed with paraformaldehyde (PFA) for immunostaining assay.

【Results】

Treatment of striatal slices with high K^+ or NMDA induced the phosphorylation of CaMKII at Thr286, MYPT1 at Thr853, and PSD-93 at Thr612 (Figure 3A–D). However, the pretreatment with Y-27632 significantly inhibited the high K^+ or NMDA-induced phosphorylation of MYPT1 and PSD-93, but not of CaMKII (Figure 3A–D). Furthermore, pre-treatment with MK-801 (NMDAR antagonist) significantly inhibited the high K^+ or NMDA-induced phosphorylation of CaMKII, of MYPT1, and PSD-93 (Supplementary Materials, Figure S2A–D). These results indicate that Rho-kinase phosphorylates PSD-93 at Thr612 and MYPT1 at Th853 downstream of NMDARs in striatal slices under conditions of NMDAR agonist-mediated CaMKII stimulation.

To identify the meaning of PSD-93 phosphorylation, the mouse striatal slices were treated with calyculin A and/or Y-27632, and an immunoprecipitation assay using an anti-PSD-93 antibody was performed. The coprecipitation of PSD-93 with PSD-95, NR1, and GluR1 was increased by treatment with calyculin A, whereas pretreatment with Y-27632 significantly inhibited these interactions (Figure 5A–D). These results suggest that Rho-kinase positively regulates the interaction of PSD-93 with PSD-95, NMDARs and AMPARs. To further explore the relationship between PSD-93 and PSD-95, the COS7 cells was cotransfected with wild-type PSD-93-PDZ3-SH3-WT, phospho-deficient PSD-93-PDZ3-SH3-T585A/T612A, or phospho-mimic mutant PSD-93-PDZ3-

SH3-T585D/T612D along with wild type Myc-PSD-95 and then stimulated with calyculin A and/or Y-27632. Treatment of COS7 cells with calyculin A increased the interaction of wild-type PSD-93-PDZ3-SH3-WT with Myc-PSD-95 compared to the control, while pretreatment with Y-27632 significantly inhibited this interaction (Figure 5E, F). The phospho-deficient mutant (PSD-93-PDZ3-SH3-T585A/T612A) showed a reduced interaction with Myc-PSD-95, and the phospho-mimetic mutant (PSD-93-PDZ3-SH3-T585D/T612D) showed an enhanced interaction with Myc-PSD-95 (Figure 5E, F). These results indicate that Rho-kinase phosphorylates PSD-93, thereby positively regulating the interaction of PSD-93 with PSD-95.

To further monitor and investigate the role of PSD-93 phosphorylation by Rho-kinase, we performed chemical LTP assay. we found that the chemical LTP induction increased the phosphorylation of MYPT1 Thr853 and PSD-93 Thr612 at 10 min and 60 min which is inhibited by pretreatment with Y-27632 (Figure 6A–C), indicating that Rho-kinase phosphorylates PSD-93 downstream of NMDARs during LTP induction. Next, we examined the localization of PSD-93 and PSD-95 in dendritic spines during LTP induction. The neurons at DIV21 were pretreated with dimethyl sulfoxide (DMSO) or Y-27632 for 20 min and incubated with glycine for 60 min to induce chemical-LTP. We found that chemical-LTP increased the dendritic spine volume but suppressed with Y-27632 pretreatment (Figure 6D, E). Moreover, we found that the colocalization of PSD-93 with PSD-95 increased after chemical LTP induction in the dendritic spines, but was significantly inhibited by pretreatment with Y-27632 (Figure 6D, F).

【Discussion】

In this study, we also found that Rho-kinase phosphorylated PSD-93 at Thr612 downstream of NMDARs in acute striatal slices (Figure 3A–D). Chemical-LTP increased the phosphorylation of PSD-93 at Thr612 in a Rho-kinase-dependent manner (Figure 6A–C). Other publications have revealed that PSD-93 deletion leads to the mislocalization of Fyn from the synaptosomal membrane. As a result, tyrosine phosphorylation of NR2A and NR2B is depleted. These findings indicate that PSD-93 acts as a membrane-anchored substrate of Fyn and plays a major role in the regulation of Fyn-mediated upregulation of NMDAR function. Furthermore, the chemical LTP induction increased dendritic spine volume and the colocalization of PSD-93 with PSD-95 in cultured striatal neurons (Figure 6D, E). Ectopic expression of PSD-93 and PSD-95 in COS7 cells resulted in an interaction between PSD-93 and PSD-95. This interaction was facilitated by the phosphorylation of PSD-93 at Thr612 and Thr585 of PSD-93 by Rho-kinase (Figure 5E, F). Taken together these results suggest that PSD-93 and PSD-95 form heterodimers in a phosphorylation-dependent manner and that the interaction contributes to LTP induction by stabilizing NMDAR localization at the plasma membrane.

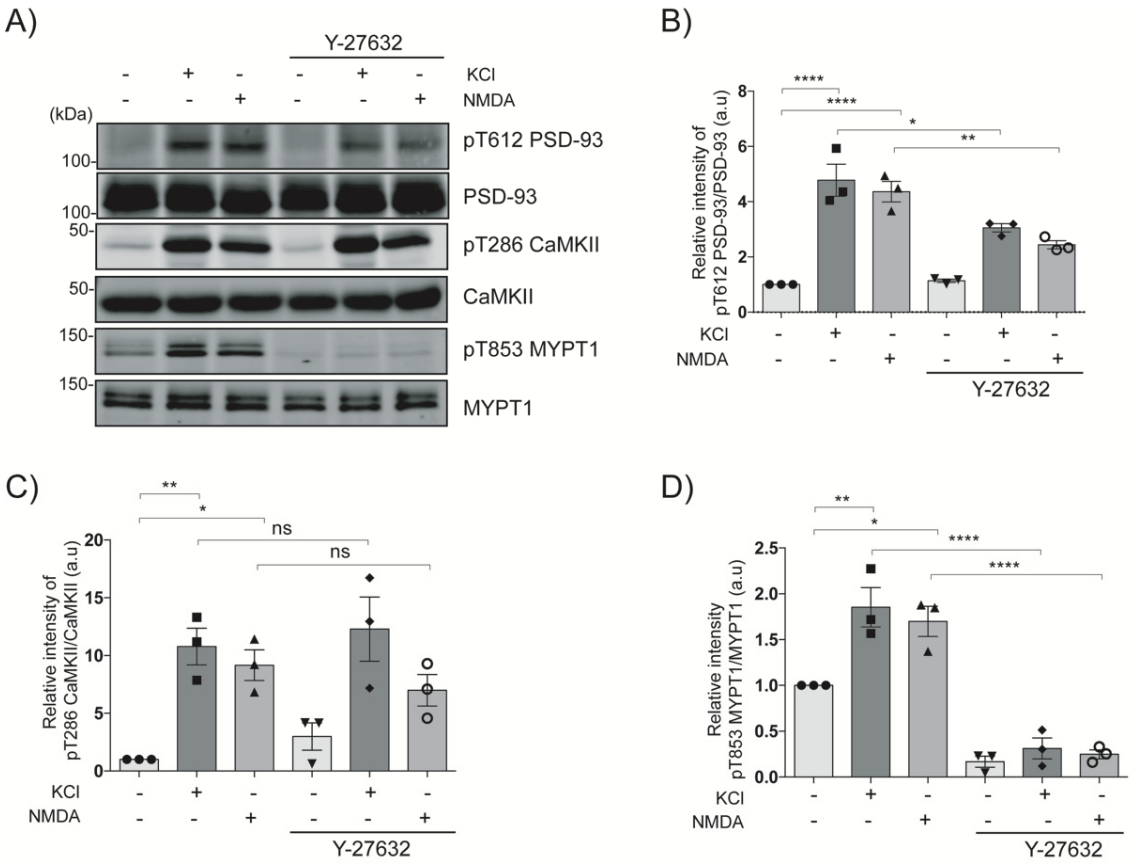

Figure 1: Rho-kinase phosphorylates PSD-93 at Thr612 in striatal slices downstream of NMDARs.
(A) Striatal slices were treated with or without the Rho-kinase inhibitor Y-27632 (20 μM for 60 min) and then treated with DMSO, or high K^+ (KCl, 40 mM) for 15 sec, or NMDA (100 μM) for 15 s. The samples were analyzed with immunoblot analysis with anti-pT612 PSD-93, anti-PSD-93, an-ti-pT286 CaMKII, anti-CaMKII, anti-pT853 MYPT1, and anti-MYPT1 antibodies. (B–D) The bar diagram shows the quantification of the immunoblot data for pT612 PSD-93, pT286 CaMKII, and pT853 MYPT1, respectively. The horizontal lines indicate the mean ± SEM of three independent experiments. *, ** and **** represent, $p < 0.05$, $p < 0.01$, $p < 0.0001$, respectively, and "ns" denotes "not significant", for Tukey's multiple comparisons test.

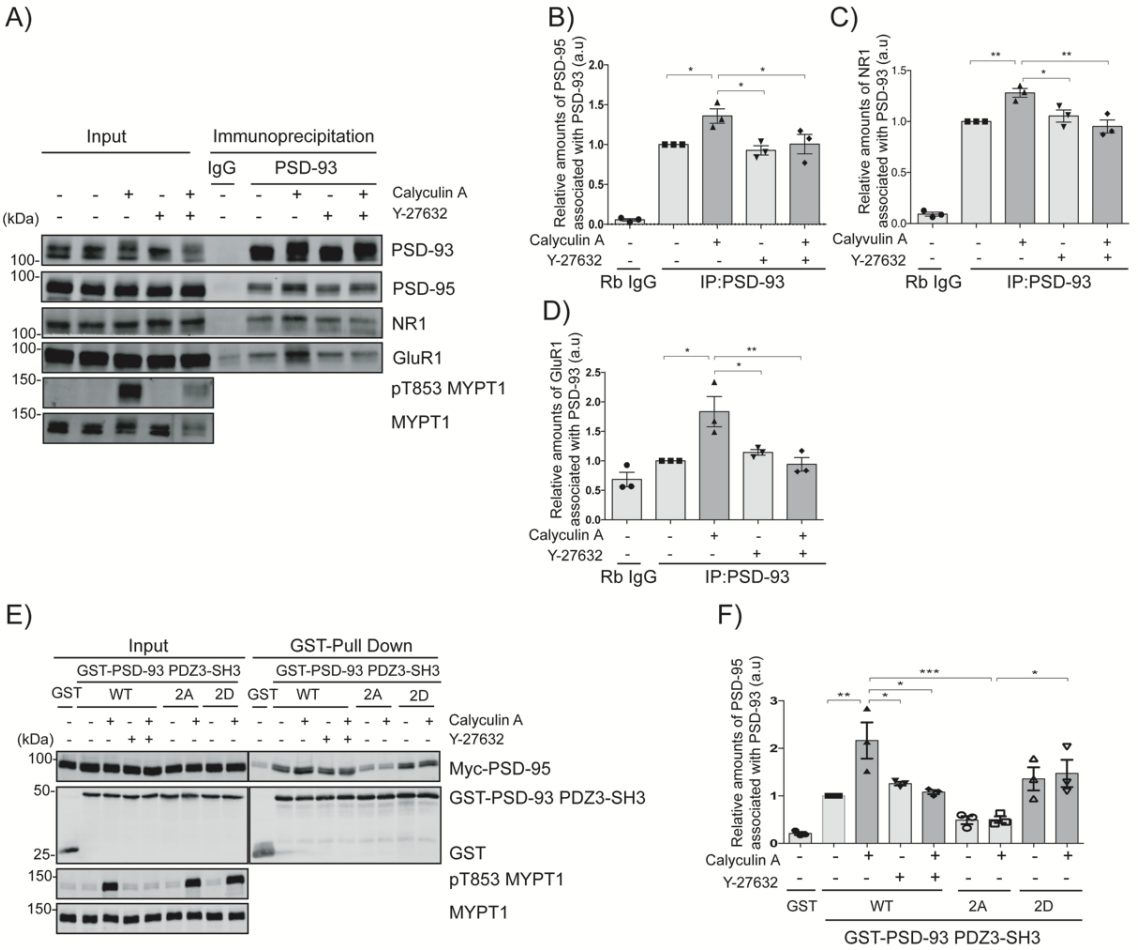

Figure 2: Rho-kinase positively regulates the interaction of PSD-93 with PSD-95, NMDARs and AMPARs.
(A) PSD-93 phosphorylation by Rho-kinase increases its interaction with PSD-95, NR1 and GluR1 in striatal slices. Striatal slices were treated with calyculin A (250 nM) for 60 min after they were pretreated with Y-27632 (20 μM) for 60 min and then immunoprecipitated using an anti-PSD-93 antibody. The precipitated proteins were subjected to immunoblot analysis with antibodies against PSD-93, PSD-95, NR1, GluR1, pT853 MYPT1, and MYPT1 antibodies. (B–D) The bar di-agram shows the statistical analysis results for the immunoblot data. The horizontal lines indicate the mean ± SEM of three independent experiments. * and ** represent $p< 0.05$ and $p< 0.01$, re-spectively, for Tukey's multiple comparisons test. (E) Rho-kinase increased the interaction of PSD-93 with PSD-95 in COS7 cells: COS7 cells were cotransfected with Myc-PSD-95 and GST-PSD-93-PDZ3-SH3 (WT, phosphodeficient and phosphomimetic mutants) and then treated with calyculin A (50 nM) for 12 min with or without pretreatment with Y-27632 (20 μM). The samples were subjected to a GST pull-down assay. (F) The bar diagram shows the quantification of the immunoblot data. The horizontal lines indicate the mean ± SEM of three independent ex-periments. *, ** and *** represent $p < 0.05$, $p < 0.01$ and $p < 0.001$, respectively, for Tukey's multiple comparisons test.

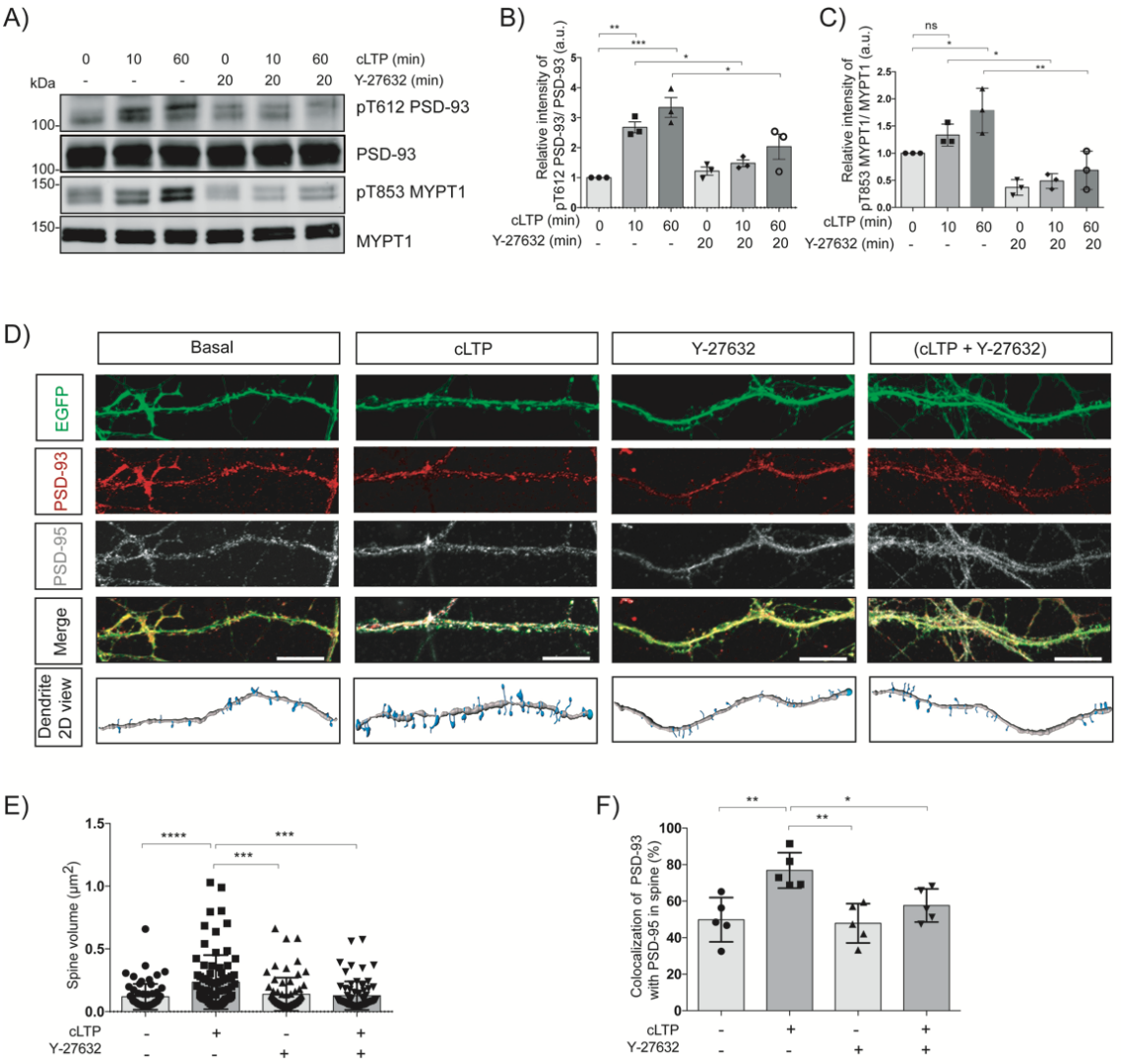

Figure 3: Chemically induced-LTP increases the Rho-kinase-mediated phosphorylation of PSD-93 and the colocalization of PSD-93 with PSD-95

(A) Chemical-LTP induces the PSD-93 phosphorylation in cultured striatal neurons. Striatal neurons were cultured until DIV21 and then neurons were treated with glycine (200 µM) after pre-treatment with the Rho-kinase inhibitor Y-27632 (20 µM). The samples were analyzed by immunoblot analysis of anti-pT612 PSD-93, anti-PSD-93, anti-pT853 MYPT1, and anti-MYPT1 antibodies. (B) (C) The horizontal lines represent the mean ± SEM of three independent experiments. *, ** and *** represent $p < 0.05$, $p < 0.01$, $p < 0.001$, respectively, and "ns" denotes "not significant", for Tukey's multiple comparisons test. (D) Colocalization of PSD-93 with PSD-95 during chemical-LTP in cultured primary striatal neurons. The neurons were cultured until DIV14 and infected with AAV-EGFP and AAV-Cre virus. After DIV21, the neurons were treated with glycine to induce chemical-LTP and the immunostaining was performed with anti-GFP (green), anti-PSD-93 (red) and anti-PSD-95 (white) antibodies. The scale bar is 10 µM. (E) (F) The horizontal lines represent the mean ± SEM of five independent experiments. *, **, *** and **** represent $p < 0.05$, $p < 0.01$, $p < 0.001$ and $p < 0.001$, respectively, for Tukey's multiple comparisons test.